

Flow-dependent directional growth of carbon nanotube forests by chemical vapor deposition

This article has been downloaded from IOPscience. Please scroll down to see the full text article.

2011 Nanotechnology 22 095303

(<http://iopscience.iop.org/0957-4484/22/9/095303>)

View [the table of contents for this issue](#), or go to the [journal homepage](#) for more

Download details:

IP Address: 115.145.209.72

The article was downloaded on 22/02/2011 at 10:51

Please note that [terms and conditions apply](#).

Flow-dependent directional growth of carbon nanotube forests by chemical vapor deposition

Hyeongkeun Kim^{1,2,4,5}, Keun Soo Kim^{2,3,4,6}, Junmo Kang²,
Young Chul Park¹, Kyoung-Yong Chun¹, Jin-Hyo Boo³,
Young-Jin Kim^{1,2}, Byung Hee Hong^{2,3,7} and Jae-Boong Choi^{1,2,7}

¹ School of Mechanical Engineering, Sungkyunkwan University, Suwon, 440-746, Korea

² SKKU Advanced Institute of Nanotechnology (SAINT) and Center for Human Interface Nano Technology (HINT), Sungkyunkwan University, Suwon, 440-746, Korea

³ Department of Chemistry, RIAN and Institute of Basic Science, Sungkyunkwan University, Suwon, 440-746, Korea

E-mail: byunghee@skku.edu and boong33@skku.edu

Received 30 November 2010, in final form 1 December 2010

Published 27 January 2011

Online at stacks.iop.org/Nano/22/095303

Abstract

We demonstrated that the structural formation of vertically aligned carbon nanotube (CNT) forests is primarily affected by the geometry-related gas flow, leading to the change of growth directions during the chemical vapor deposition (CVD) process. By varying the growing time, flow rate, and direction of the carrier gas, the structures and the formation mechanisms of the vertically aligned CNT forests were carefully investigated. The growth directions of CNTs are found to be highly dependent on the nonlinear local gas flows induced by microchannels. The angle of growth significantly changes with increasing gas flows perpendicular to the microchannel, while the parallel gas flow shows almost no effect. A computational fluid dynamics (CFD) model was employed to explain the flow-dependent growth of CNT forests, revealing that the variation of the local pressure induced by microchannels is an important parameter determining the directionality of the CNT growth. We expect that the present method and analyses would provide useful information to control the micro- and macrostructures of vertically aligned CNTs for various structural/electrical applications.

 Online supplementary data available from stacks.iop.org/Nano/22/095303/mmedia

1. Introduction

Carbon nanotubes (CNTs) have been intensively studied because of their outstanding physical properties and their potential applications to micro-electronic devices [1–6]. The structural perfection of CNTs enables ~8 times larger electrical conductivity and ~10 times higher thermal conductivity than those of copper [7–12]. Recently, the potential use of vertically aligned CNT electrodes for

ultrafast highly integrated digital circuits has attracted much attention owing to the excellent electrical and structural properties [13–18]. However, the gas flow during the CVD process sometimes causes unexpected deformation of CNT forests, resulting in the degradation of electrical and structural properties [19, 20]. Therefore, a precise control technique minimizing the structural defects are essential to enhance the growth quality of CNT forests.

Endo *et al* [21] utilized a computational fluid dynamics (CFD) model to predict the growth rate of multiwalled CNTs (MWCNTs), which well matches with the experimental results. Nasibulin *et al* [22] also reported that the growth patterns of multiwalled CNTs can be explained by CFD calculations considering temperature, velocity profiles, and

⁴ These authors contributed equally to this work.

⁵ Present address: Electronic Materials & Device Research Center, Korea Electronics Technology Institute (KETI), Seongnam, 463-816, Korea.

⁶ Present address: Department of Physics, Columbia University, New York, NY 10027, USA.

⁷ Authors to whom any correspondence should be addressed.

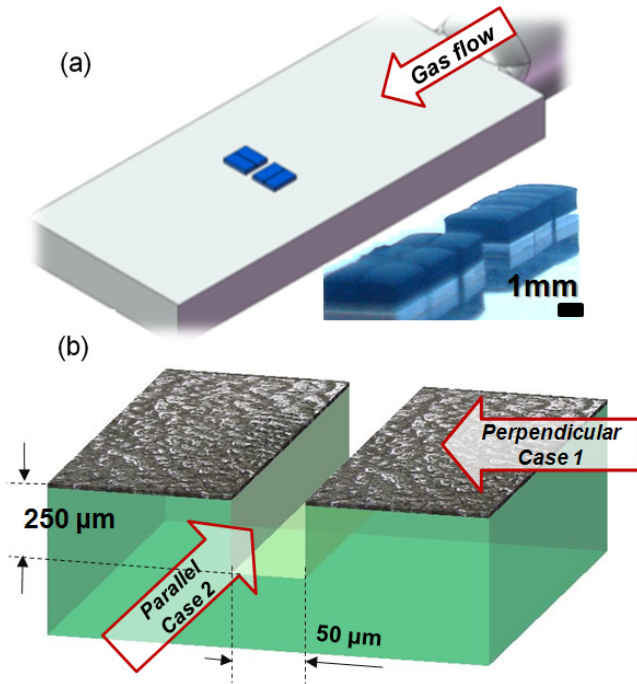


Figure 1. Illustration of the experimental setup (a) schematic and photographic (inset) images of vertically aligned CNTs, (b) schematic of the microchannel design fabricated by a silicon dicer.

(This figure is in colour only in the electronic version)

mixing conditions inside a CVD reactor. However, the previous reports [20, 23] did not consider the influence of numerous parameters such as the flow direction, flow rate, reaction temperature, reaction time, and substrate geometry. Thus, we report the importance of the above factors controlling the vertical structures of the CNT, based on both experimental and numerical analyses. First, we experimentally examined the relationship between the flow direction and the deformation of vertically aligned CNTs, and then numerically analyzed the gas flow around the microchannel using a CFD model to explain the growth mechanism.

2. Experimental details

Figure 1 shows the microchannel design fabricated by a dicing saw (DASCO: DAC552). The substrate was cut into 3 mm × 3 mm square pieces. A crevice with a width of 50 μm and depth of 250 μm was made at the center of the substrate with a dicing saw. The carrier gas flowed in different (perpendicular and parallel) directions through the microchannel. The detailed experimental procedure used to fabricate the CNTs has previously been described [24–27]. The flow rate and reaction time are described in table 1.

We also applied the CFD model to evaluate the growth mechanism of CNT forests. In particular, the CFD model is helpful in interpreting nanotube growth rates, transport rates and reaction mechanisms [21]. A three-dimensional design program (Solidworks) was used to model the fluid domain of the CVD for the CFD modeling. A mesh was created for the fluid domain using ICFM CFD from CFX [28]. In order to

Table 1. List of experimental conditions.

Conditions	Gas flow rate (sccm)			Reaction time (min)	Growth temp. (K)
	H ₂	C ₂ H ₄	Ar		
I	50	30	150	5/10/20	1023
II	50	30	170	20	1023
III	50	30	190	20	1023

reduce the analysis time for the mesh formation, a symmetric model was assumed as the width of the microchannel. To investigate the viability of the CFD, the Reynolds number was first calculated using equation (1) to verify the presence of laminar flow [29].

$$Re = \rho UL/\mu \quad (1)$$

where μ is the viscosity, ρ the density, U the average velocity and L the tube inner diameter. The calculated Reynolds numbers were 5.3 around the substrate holder in the CVD chamber. Then, the Knudsen number (K_n) was obtained using equation (2) to check whether the continuum flow and no-slip wall boundary can be applied to the CFD model [29].

$$K_n = \lambda/h. \quad (2)$$

The Knudsen number is defined as the ratio of the mean free path (λ) over a characteristic geometry length (h). The calculated Knudsen number was 0.00624. Upon calculation of the Knudsen number, which was found to fall in the range ($0 \leq K_n \leq 1$), both the continuum flow and no-slip boundary conditions were applied to the numerical analysis [29]. Here, the mean free path depends on both temperature and pressure, so the mean free path was corrected using equation (3) for a chamber temperature of 1023 K [30].

$$\lambda(T, P) = \lambda(T_0, P_0) \times \left(\frac{P_0}{P}\right) \times \left(\frac{T}{T_0}\right) \times \left(\frac{1 + \frac{S}{T_0}}{1 + \frac{S}{T}}\right) \quad (3)$$

where $\lambda(T_0, P_0)$ is the mean free path of Ar at atmospheric conditions (70.4 nm [29, 30]), h the dimension of the flow field (50 μm), T the growth temperature (1023 K), T_0 the reference room temperature (293 K), P the gage pressure, P_0 the reference pressure ($P = P_0$), and S the Sutherland coefficient (141.4 [30]). The calculated mean free path was 312 nm.

3. Results and discussions

Figure 2 shows SEM images of the microchannel gaps on the microstructures of the vertically aligned CNTs with different flow directions and rates, under the same growth temperature (1023 K). Figures 2(a)–(c) show the case with the flow direction of the carrier gas perpendicular to the microchannel (case 1). The gas flow rate was gradually increased from 20 to 150 sccm over a period of 20 min. Figures 2(d)–(f) show the SEM images of the microstructures of the vertically aligned CNTs with the parallel flow direction to the microchannel (case 2) under the same conditions as above. The synthesis of the CNTs was repeated three times at the same experimental

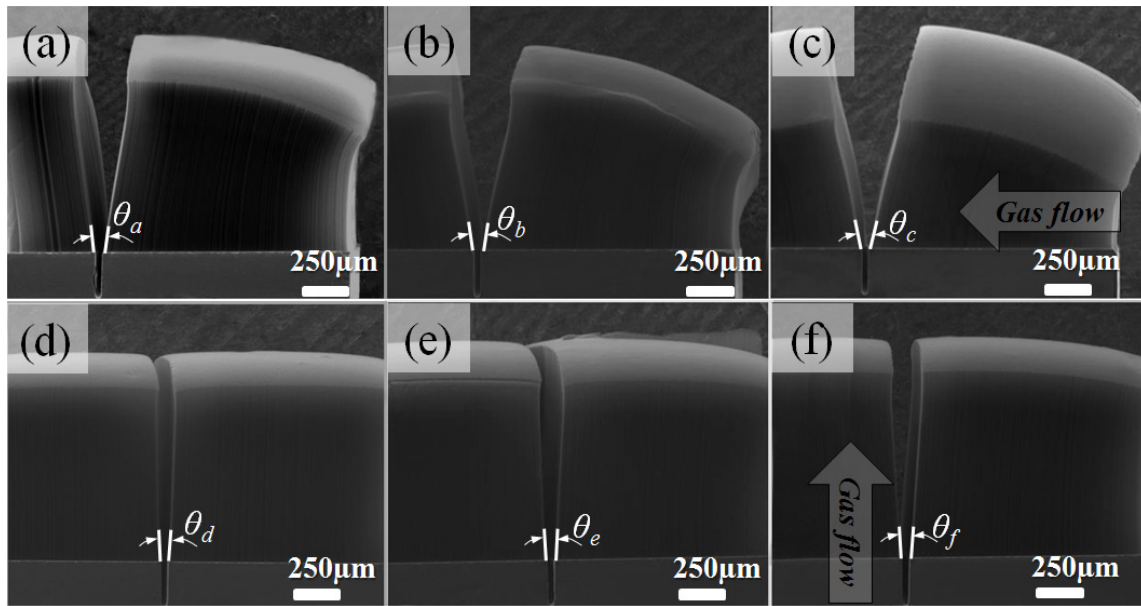


Figure 2. SEM images of CNT microstructures for different flow rates of carrier gas but with the same growing time of 20 min. Case 1 (gas flow perpendicular to the microchannel): $\theta_a = 11^\circ \pm 0.5^\circ$, $\theta_b = 15^\circ \pm 0.5^\circ$, $\theta_c = 20^\circ \pm 0.5^\circ$ for (a) Ar (150), (b) Ar (170), (c) Ar (190 sccm), respectively. Case 2 (gas flow parallel to the microchannel): $\theta_d = 4^\circ \pm 0.4^\circ$, $\theta_e = 5^\circ \pm 0.4^\circ$ and $\theta_f = 6^\circ \pm 0.4^\circ$ for (d) Ar (150), (e) Ar (170), (f) Ar (190 sccm), respectively.

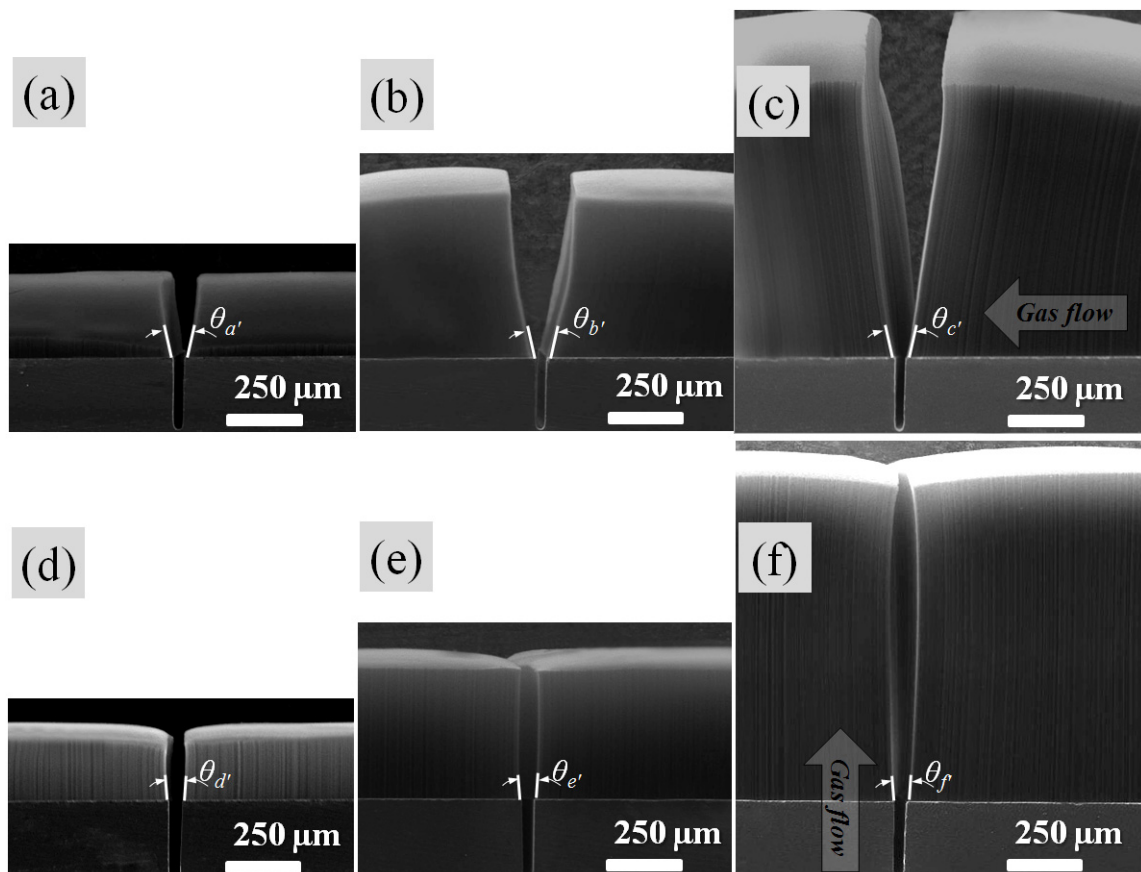


Figure 3. SEM images of CNT microstructures as a function of growth times, under the constant gas flow rates with H_2 (50 sccm), C_2H_4 (30 sccm), Ar (150 sccm), respectively. $\theta_{a'} = \theta_{b'} = \theta_{c'} = 11^\circ \pm 0.5^\circ$, $\theta_{d'} = \theta_{e'} = \theta_{f'} = 4^\circ \pm 0.4^\circ$. Case 1: perpendicular gas flow to the microchannel for: (a) 5 min, (b) 10 min and (c) 20 min. Case 2: parallel gas flow to the microchannel for: (d) 5 min, (e) 10 min and (f) 20 min. The detailed analyses of the rate and size-dependences on the CNT growths are described in the supplementary data (available from: stacks.iop.org/Nano/22/095303/mmedia).

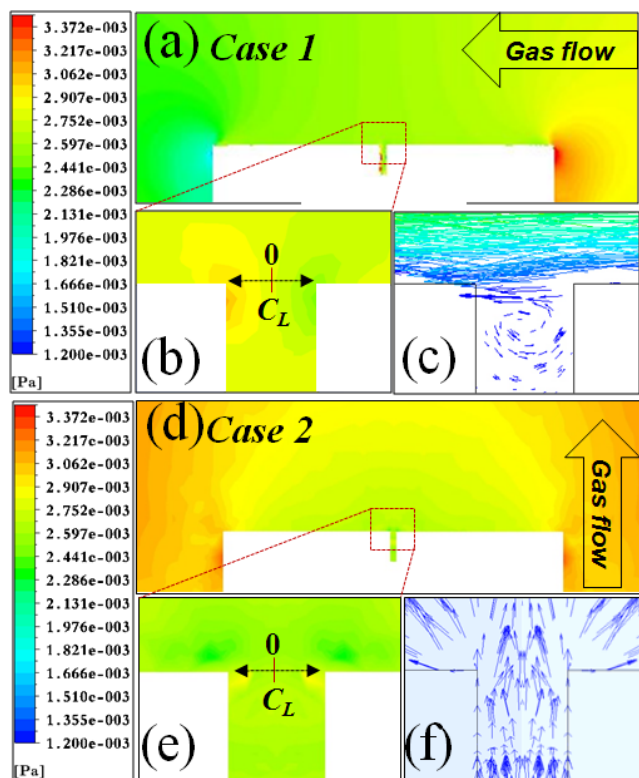


Figure 4. The results of the simulations: (a), (b) pressure contour and (c) velocity vortex of the microchannel (case 1; gas flow perpendicular to the microchannel). (d), (e) pressure contour and (f) velocity vortex of the microchannel (case 2; gas flow parallel to the microchannel).

conditions to check the reproducibility. We observed that the flow directions were very important for the creation of microchannel flows in vertically aligned CNTs growth whereas the flow rates were not. In comparing the two cases, there is an obvious change in the microchannel gap for case 1, while the microchannel gap was almost the same regardless of the flow rate for case 2. For case 1, the initial angle of the microchannel is $11^\circ \pm 0.5^\circ$, which is almost three times as large as case 2. The angle of the microchannel also increases from 11° to $20^\circ \pm 0.5^\circ$ according to the increase in gas supply with a fixed growing time. For case 2, the difference in the microchannel gap is almost constant with different flow rates. Consequently, it has been found that the formation of vertically aligned CNTs using CVD with microchannel-substrates depends greatly on the flow directions and much less on the flow rates, which indicates that the flow directions have high impact on this study. Based on case 1 and case 2, we considered that a more precise gas flow control is required to obtain uniform CNT forests because the synthesis of super-growth vertically aligned CNTs is needed to minimize the edge bending effect due to the microchannel gap [31, 32].

To examine the relation between the geometry-related flow and growth time for vertically aligned CNTs, we varied the reaction time (5/10/20 min), as shown in figure 3. For case 1, it is observed that a edge bending of the parabolic structure is initially created, while the edge bending phenomenon was not affected by the growth time for case 2.

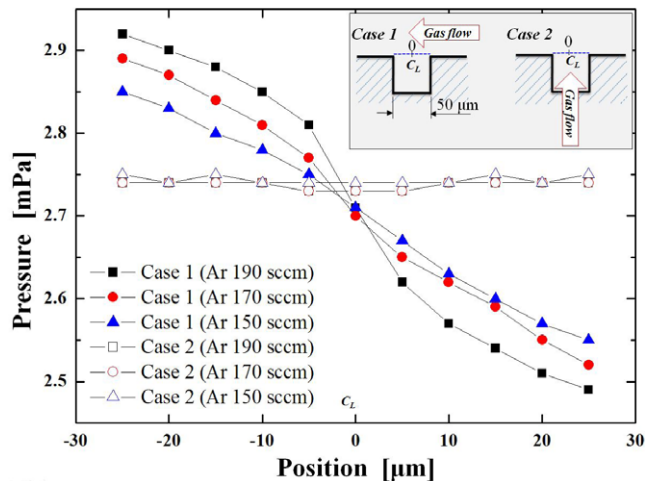


Figure 5. The results of the pressure distributions of the sectional view on the microchannel (case 1 and case 2) from simulations.

The length of the CNTs gradually increases with a longer growth time. However, the microchannel gaps from the formation of vertically aligned CNTs remain constant at $11^\circ \pm 0.5^\circ$ ($\theta_{ar} = \theta_{br} = \theta_{cr}$) for case 1 and at $4^\circ \pm 0.4^\circ$ ($\theta_{dr} = \theta_{er} = \theta_{fr}$) for case 2 irrespective of the growth time, indicating that the shape of the CNT forest is determined by the initial microchannel flow. It has been reported that an increase in the carbon source near the vicinity of the microchannel leads to a discrepancy in the height of the CNT forests [17]. This kind of phenomenon results in the breaking of the energy valence of the CNTs along with a deterioration in bending and stranding at the edges. In this report we considered that the flow direction is the most important factor to affect the super-growth of vertically aligned CNTs, as far as the discrepancy in the CNT height due to both bending and stranding at the edges.

The growth mechanism of the CNT forests with respect to the flow rate and the direction of gas supply were investigated through numerical analysis. Figures 4(a), (b) and (d), (e) show the pressure contours in the proximity of the microchannel for case 1 and case 2, respectively. The microchannel pressure contour detail view for case 1 is shown in figure 4(b).

We confirm that the pressure contour generates the opposite pressure based on the center line (C_L). In the same manner, the microchannel pressure contour detail view for case 2 is shown in figure 4(e) and indicates the pressure contour of the microchannel mid-point cross-sectional area.

We clearly found that the contour color is almost unchanged, which signifies that the variation in the pressure around the microchannel is insignificant. Moreover, in figures 4(c) and (f), the velocity vortices for cases 1 and 2 are shown. It is found that a different vortex arises due to the pressure variation in the microchannel aided edge bending. In particular, as is shown in figure 4(c), the generation of the circulation vortex is found in the microchannel, which indicates the typical grooved-channel flow [29].

The pressure variations across the microchannels are illustrated in figure 5. The maximum pressure variations for case 1 and case 2 were 0.43 and 0.01 mPa, respectively. Case 1 demonstrates larger pressure variations than case 2 does. This

numerical analysis reveals that the pressure variations across the cross-section of the microchannel are significant on the edge bending for case 1, which is highly consistent with the experimental results.

4. Conclusions

Experimental and numerical analyses were employed to investigate the effect of microchannel flow on the formation of vertically aligned CNT forests. We found that the structure deformation of vertically aligned CNT forests was very dependent on geometry-related flows that introduced variations in the microchannel gap. However, the flow rate and the growth time were insignificant for the structure deformation of CNT forests. Numerical analysis revealed that the main parameter for the edge bending of vertically aligned CNT forests was the pressure variation occurring near the CNT forests.

We concluded that the direction of gas flow is a primary factor in the structural deformation of vertically aligned CNT forests, which in turn gives rise to the edge bending effect. Consequently, the fine control of the flow conditions is needed to minimize the edge bending effects for the synthesis of super-growth vertically aligned CNTs. Many other parameters, such as the reaction temperature, chemical reaction and substrate geometry must also be considered to synthesize good super-growth vertically aligned CNT forests while decreasing structure deformation such as edge bending. As further research work, we plan to grow 3D CNT forest structures for the electrode material of electronic circuitry and packaging systems using precise numerical control of the small pressures.

Acknowledgments

This work was supported by the WCU (World Class University) program through the Korea Science and Engineering Foundation funded by the MEST (Ministry of Education, Science and Technology) (R33-2008-000-10027, R33-2008-000-10138) and the National Research Foundation of Korea Grant funded by the Korean Government (MEST) (KRF-2008-313-D00131, KRF-2008-005-J00702, 2010-0015035, 2010K001066). We would also like to thank MEST and the Ministry of Knowledge Economy (MKE) through the fostering project HUNIC.

References

- [1] Wong E W, Sheehan P E and Lieber C M 1997 *Science* **277** 1971
- [2] Walters D A, Ericson L M, Casavant M J, Liu J, Colbert D T, Smith T A and Smalley R E 1999 *Appl. Phys. Lett.* **74** 3803
- [3] Yu M F, Files B S, Arepalli S and Ruoff R S 2000 *Phys. Rev. Lett.* **84** 5552
- [4] Hasegawa K, Noda S, Sugime S, Kakehi K, Maruyama S and Yamaguchi Y 2008 *J. Nanosci. Nanotechnol.* **8** 6123
- [5] Robertson J, Hofmann S, Cantoro M, Parvez A, Ducati C, Zhong G, Sharma R and Mattevi S 2008 *J. Nanosci. Nanotechnol.* **8** 6105
- [6] Datsyuk V, Kalyva M, Papagelis K, Parthenios J, Tasis D, Siokou A, Kallitsis I and Galiotis C 2008 *Carbon* **46** 833
- [7] Pop E, Mann D, Wang Q, Goodson K and Dai H 2006 *Nano Lett.* **6** 96
- [8] Wang J and Wang J S 2006 *Appl. Phys. Lett.* **88** 111909
- [9] Ouyang M, Huang J L and Lieber C M 2002 *Acc. Chem. Res.* **35** 1018
- [10] Hone J, Whitney M, Piskoti C and Zettl A 1999 *Phys. Rev. B* **59** R2514
- [11] Yao Z, Kane C L and Dekker C 2000 *Phys. Rev. Lett.* **84** 2941
- [12] Oh Y S, Choi J B, Kim Y J, Kim K S and Baik S 2007 *Scr. Mater.* **56** 741
- [13] Hayamizu Y H, Yamada T K, Mizuno K H, Davis R C, Futaba D N, Yumura M and Hata K 2008 *Nat. Nanotechnol.* **3** 289
- [14] Wei B Q, Vajtai R and Ajayan P M 2001 *Appl. Phys. Lett.* **79** 1172
- [15] Patole S P, Patole A S, Rhen D S, Shahid M, Min H, Kang D J, Kim T-H and Yoo J-B 2009 *Nanotechnology* **20** 315302
- [16] Bernadette M Q and Serge G L 2006 *Adv. Mater.* **18** 855
- [17] Pint C L, Bozzolo G and Hauge R 2008 *Nanotechnology* **19** 405704
- [18] Li J, Ye Q, Cassell A, Ng H T, Stevens R, Han J and Meyyappan M 2006 *Appl. Phys. Lett.* **82** 2491
- [19] Hart A J 2006 *PhD Thesis* Massachusetts Avenue Cambridge USA, Massachusetts Institute of Technology
- [20] Han J H, Graff R A, Welch B, Marsh C P, Franks R and Strano M S 2008 *ACS Nano* **2** 53
- [21] Endo H, Kuwana K, Saito K, Qian D, Andrews R and Grulke E A 2004 *Chem. Phys. Lett.* **387** 307
- [22] Nasibulin A G, Moisala A, Brown D P, Jiang H and Kauppinen E I 2005 *Chem. Phys. Lett.* **402** 227
- [23] Zhu L, Xu J, Xiao F, Jiang H J, Hess D W and Wong C P 2007 *Carbon* **45** 344
- [24] Kim H, Lee C S, Choi J B, Chun K Y, Kim Y J and Baik S 2009 *J. Kor. Phys. Soc.* **54** 1006
- [25] Patole S P, Kim H, Choi J B, Kim Y J, Baik S and Yoo J B 2010 *Appl. Phys. Lett.* **96** 094101
- [26] Kim H, Chun K Y, Choi J B, Kim Y J and Baik S 2010 *J. Nanosci. Nanotechnol.* **10** 3362
- [27] Kim H, Kang J, Kim Y J, Hong B H, Choi J B and Iijima S 2010 *J. Nanosci. Nanotechnol.* **11** 470
- [28] Kim H T, Rhee B W and Park J H 2008 *Nucl. Eng. Des.* **238** 522
- [29] Karniadakis G, Beşkök A and Aluru N R 2005 *Microflows and Nanoflows: Fundamentals and Simulation* (New York: Springer)
- [30] Daniel J R 1990 *J. Aerosol Sci.* **21** 161
- [31] Hata K J, Futaba D N, Mizuno K, Namai T, Yumura M and Iijima S 2004 *Science* **306** 1362
- [32] Hart A J and Slocum A H 2006 *J. Phys. Chem. B* **110** 8250